Propeller-Wing Integration for Minimum Induced Loss

Ilan Kroo*
Stanford University, Stanford, California

An analysis of propeller-wing combinations in inviscid incompressible flow reveals some of the fundamental interactions which affect the performance of an installed propulsion system. A generalized version of Munk's stagger theorem is used in a rapid, approximate calculation of optimal lift distributions and installed efficiency. Results indicate that the distribution of lift over the wing which maximizes overall efficiency differs markedly from elliptic loading. Swirl recovery by the wing leads to increments in net propeller efficiency of 6% in example cases. The maximum installed efficiency is computed for single-rotation (up-inboard and up-outboard designs) and counter-rotating systems. Results suggest that some of the performance advantages attributed to counter-rotation may be less dramatic for well-integrated wing-propeller designs than for isolated systems.

Nomenclature

A_n = amplitude of nth harmonic of wing lift
AR = wing aspect ratio
b = wingspan
c = wing chord
C_L = wing lift coefficient
C_T = thrust coefficient, $= \pi^2 T/\rho\omega^2 R^4$
D = drag
I_u, I_w = definite integrals, Eqs. (10) and (11), respectively
J = advance ratio, $= \pi U_\infty/\omega R$
l = section lift
L = lift
N = number of blades
Obj = objective function
Q = propeller torque
R = propeller radius
r = radial coordinate
T = thrust
U_∞ = freestream velocity
u = axial perturbation velocity
V = induced velocity
v_t = tangential induced velocity
w = induced downwash
x = streamwise coordinate
y = spanwise coordinate
y_{prop} = spanwise location of propeller
Γ = circulation
θ = dimensionless spanwise coordinate
κ = Goldstein's radial velocity correction
λ = Lagrange multiplier
ρ = density

Subscripts

int = interference component
w = wing
p = propeller

Introduction

EFFICIENT propeller-wing integration has remained an important and difficult problem, made perhaps more important, and certainly more difficult, with the introduction of propfans. Many aspects of the problem have been addressed, from fundamental discussions by Glauert[1] to very recent analyses[2-5] which include design optimization in the transonic regime. In this paper, one aspect of the interaction between propeller and wing is examined: the interference between thin wing and propeller in inviscid, incompressible, quasisteady flow. Although the idealizations made here are extreme (especially for high-speed propellers), the simple analysis produces several useful results which more detailed and complete methods may extend.

The specific problem addressed herein is the computation of net thrust for a propeller-wing combination with the wing designed to maximize this quantity. Wing lift distributions which best exploit the axial and rotational velocities in the slipstream are computed for configurations with propellers located behind the wing. The calculated lift distribution is that which produces the most favorable effect on propeller performance.

Approach

Stagger Theorem for Propellers

The simplified model of wing and propeller is shown in Fig. 1. The propeller sheds a helical wake and the wing wake is assumed flat; the effects of wake rollup and slipstream contraction are excluded from this analysis. The mutual induced velocities on wing and propeller could be computed using available lifting surface methods and the optimal distribution of circulation computed as discussed in Ref. 6 for multiple lifting surface configurations. However, the analysis is simplified greatly by the stagger theorem of Munk[7] which has been usefully applied to wing-tail combinations, but which also is applicable to propeller-wing combinations. This generalized version of the stagger theorem asserts that *the net force in the streamwise direction is independent of the streamwise position of surfaces with a given circulation distribution*. Thus, the optimal circulation distribution may be computed with the propeller far upstream of the wing, eliminating the computation of velocities induced by the wing on the propeller and by the propeller's bound vorticity on the wing. More interestingly, the theorem implies that the effect of the propeller slipstream on the wing-induced drag is identical to the effect of the wing wake on the thrust of an aft-mounted propeller. The independence of induced drag and propeller thrust with longitudinal position may be derived from the following considerations.

The drag induced by propeller-wing interference (with fixed circulation distribution) is

$$D_{int} = \int_{span} 2\bar{w}_p \rho \Gamma_w dy$$

Presented as Paper 84-2470 at the AIAA/AHS/ASEE Aircraft Design Systems and Operations Meeting, San Diego, CA, Oct. 31-Nov. 2, 1984; received Sept. 6, 1985; revision received Feb. 10, 1986.

*Assistant Professor, Department of Aeronautics and Astronautics. Member AIAA.

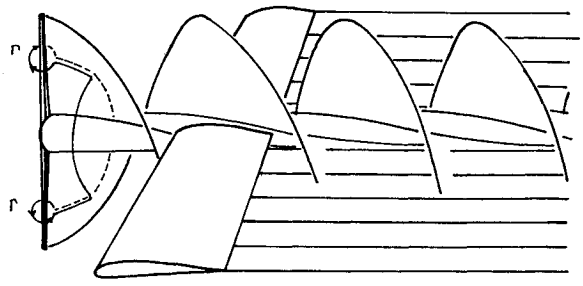

Fig. 1 Idealized propeller-wing model.

where $2\bar{w}_p$ is the average downwash induced on the wing by propeller swirl. $\bar{w}_p$ might be expected to vary with both r, the radial coordinate measured from the propeller center, and x, the streamwise distance from the propeller plane. However, the integral of $V\cdot dl$ around the contour shown in Fig. 1 vanishes since it encloses no circulation. Thus,

$$\oint V\cdot dl = 2\pi r(2\bar{w}_p) + N\Gamma_p(r) = 0$$

$$2\bar{w}_p = N\Gamma_p/2\pi r$$

so

$$D_{\text{int}} = \frac{N\rho}{2\pi}\int_{\text{span}} \frac{\Gamma_w\Gamma_p}{r(y)}dy = \frac{N\rho}{2\pi}\int_0^R \frac{\Gamma_p}{r}(\Gamma_w(r)-\Gamma_w(-r))dr \tag{1}$$

Thus, the average swirl and, hence, the induced interference are independent of x as long as the propeller is placed forward of the wing. If the propeller plane is downstream of the wing, the corresponding integral path yields

$$\bar{w}_p = 0$$

so there is no interference drag induced on the wing in this case. However, the wing produces a net interference thrust due to its interaction with the propeller. The thrust of a propeller with fixed circulation is given by

$$T = \int_{\text{prop}} N\rho\Gamma_p(\omega r - \bar{v}_t)dr$$

so, the thrust induced by interference is

$$T_{\text{int}} = \int_{\text{prop}} N\rho\Gamma_p(-\bar{v}_{t_w})dr$$

where V_{t_w} is the average tangential velocity at radius r induced by the wing. However, the average tangential velocity is related to the circulation it encloses:

$$2\pi r\bar{v}_{t_w} = \Gamma_w(r) - \Gamma_w(-r)$$

so,

$$D_{\text{int}} = \frac{N\rho}{2\pi}\int_{\text{span}} \frac{\Gamma_w\Gamma_p}{r(y)}dy = \frac{N\rho}{2\pi}\int_0^R \frac{\Gamma_p}{r}(\Gamma_w(r)-\Gamma_w(-r))dr \tag{2}$$

which is identical to Eq. (1).

Propeller-Induced Velocities

In order to examine quantitatively the effect of the propeller slipstream on wing induced drag, it is necessary to determine the axial and tangential velocities in the slipstream. This may be based on experimental data, detailed analysis, or approximate calculations. For illustrative purposes, simple results based on minimum induced-loss propeller design and Goldstein's analysis[8] yield the required values.

The induced velocities may be computed from the equations for linear and axial momentum change which may be expressed in terms of the thrust and torque per unit radius as

$$T' \equiv \frac{dT}{dr} = 2\pi r\rho(U_\infty + u)2u\kappa \tag{3}$$

$$Q' \equiv \frac{dQ}{dr} = 2\pi r\rho(U_\infty + u)2v_t r\kappa \tag{4}$$

where $2u$ is the axial induced velocity far downstream and $2v_t$ is the tangential velocity behind the propeller. These are combined with similar relations based on circulation:

$$T' = N\rho\Gamma_p(\omega r - v_t) \tag{5}$$

$$Q' = N\rho\Gamma_p(U_\infty + u)r \tag{6}$$

The final condition required to determine the five unknowns at each radial station is the condition for minimum induced loss. This relation is most easily derived by the method of restricted variations (cf., Refs. 9 and 10). Consider a variation of Γ_p about the solution for minimum loss which does not change the thrust:

$$\delta T = N\rho\delta\Gamma_1(\omega r_1 - v_{t_1}) + N\rho\delta\Gamma_2(\omega r_2 - v_{t_2}) = 0$$

$$\delta Q = N\rho\delta\Gamma_1(U_\infty + u_1)r_1 + N\rho\delta\Gamma_2(U_\infty + u_2)r_2 = 0$$

Thus,

$$r(U_\infty + u)/(\omega r - v_t) = \text{constant} \tag{7}$$

The above expressions consist of $5n$ equations in $5n+1$ unknowns (with n the number of stations at which the values are to be determined). The final equation is provided by specifying the desired thrust or power.

Optimal Wing Lift Distribution

Once the induced velocities associated with the propeller slipstream are determined, it is possible to solve explicitly for the wing lift distribution with minimum drag.

The distribution of circulation is represented by a Fourier series as

$$\rho U_\infty\Gamma = \frac{4}{\pi b}\sum_n A_n \sin n\theta \tag{8}$$

where θ is given by

$$y = (b/2)\cos\theta$$

With propeller-induced velocities of u and w_p the section lift is

$$l = \frac{4}{\pi b}\sum_n A_n \sin n\theta(1+u) \tag{9}$$

and the total lift is

$$L = \frac{4}{\pi b}\sum_n A_n\int_{-b/2}^{b/2} \sin n\theta(1+u)dy \equiv \frac{4}{\pi b}\sum_n A_n I_{un} \tag{10}$$

The expression for drag is just that obtained from finite wing theory along with an interference term:

$$D = \frac{1}{q\pi b^2}\sum_n nA_n^2 + \frac{4}{\pi b}\sum_n A_n\int_{-b/2}^{b/2} \sin n\theta w_p dy$$

$$\equiv \frac{1}{q\pi b^2}\sum_n nA_n^2 + \frac{4}{\pi b}\sum_n A_n I_{wn} \tag{11}$$

For minimum drag with fixed lift, the objective function

$$\text{Obj} = D + \lambda\left(L - \frac{4}{\pi b}\sum_n A_n I_{un}\right) \tag{12}$$

is introduced with a Lagrange multiplier λ, and the desired lift L. The optimality condition, $\partial \text{Obj}/\partial A_i = 0$, together with the constraint equation leads to an expression for the harmonic amplitudes:

$$A_n = \frac{\rho U_\infty b}{n}\left[\left(\frac{\pi L}{4\rho {U_\infty}^2} + \sum_j \frac{I_{uj} I_{wj}}{j}\right)\left(I_{un} \Big/ \sum_j \frac{{I_{uj}}^2}{j}\right) - I_{wn}\right] \tag{13}$$

Substitution into Eq. (11) then yields the drag.

Results

Propeller Analysis

The minimum induced loss propeller analysis was applied to a conventional propeller with four blades at an advance ratio of $J = 1.57$, and to a propeller more representative of a propfan with eight blades at $J = 3.14$. The propulsive efficiency is shown in Fig. 2. Inviscid efficiency is plotted vs the parameter $(8/\pi)(C_T/J^2)$. (Comparison at equal values of this parameter is equivalent to a comparison at equal values of aircraft drag coefficient and propeller diameter.)

The increasingly important effect of swirl loss as the advance ratio is increased is evident from this figure. At a typical value of C_T ($C_T = 0.387$, $(8/\pi)(C_T/J^2) = 0.1$ with $J = 3.14$) a 7% efficiency loss due to swirl is predicted. At $J = 3.8$ this penalty rises to 10%, in good agreement with other experimental and computational results.[5] Thus, although the effect is by no means negligible for conventional propellers, it is of greater importance for highly loaded propfans.

The distribution of propeller-induced velocity is shown in Fig. 3 for one example design condition. In agreement with measured values (cf., Ref. 5), swirl angles of 5-6 deg are predicted in the slipstream of a propfan at cruise conditions. The calculated results differ from actual slipstream characteristics mainly in that the effect of nacelle and hub are neglected; this has no effect on the fundamental results of the analysis. This velocity distribution was then used to compute the wing lift distribution for minimum drag.

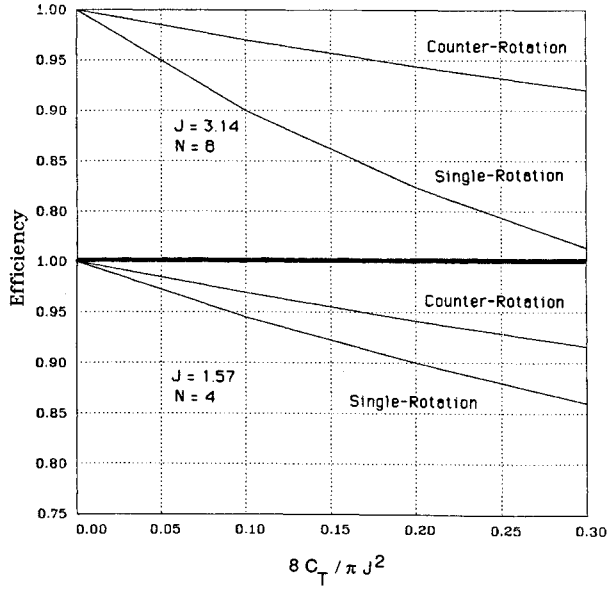

Fig. 2 Effect of advance ratio and thrust coefficient on swirl loss.

Optimal Wing Lift Distribution

The optimal spanwise distribution of wing lift, computed as discussed in the previous section, is shown in Fig. 4. In this case the aspect ratio 10 wing is located behind two 8-bladed propellers each with $J = 3.14$ and $C_T = 0.387$. The propellers are located at 40% of the semispan with a diameter-to-span ratio of 0.15.

The appearance of higher harmonics in the optimum solution is caused by both tangential and axial induced velocities and results in lift distributions that, as shown here, may depart dramatically from the "clean wing" distribution. In this case the wing behaves somewhat like a turbine stator, removing rotational energy from the slipstream. This is not to imply that an untwisted wing will naturally assume the optimal lift distribution in the presence of the propeller slipstream. In Ref. 3 the lift distribution is permitted to vary from the clean wing distribution to the extent that the slipstream produces changes

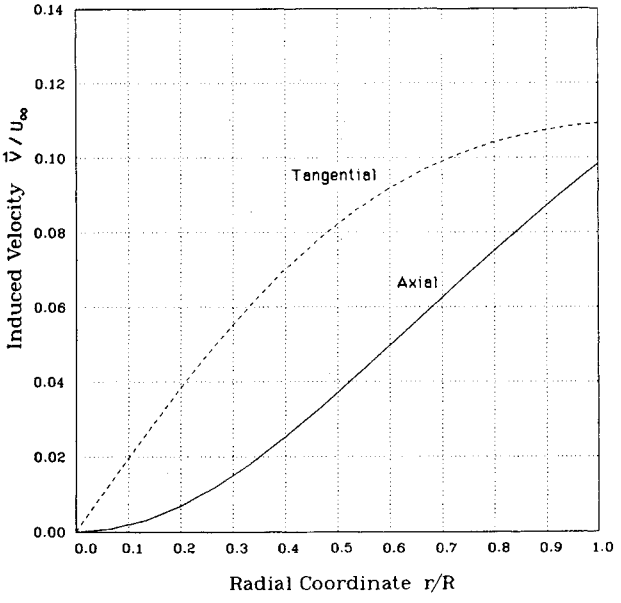

Fig. 3 Propeller-induced velocities.

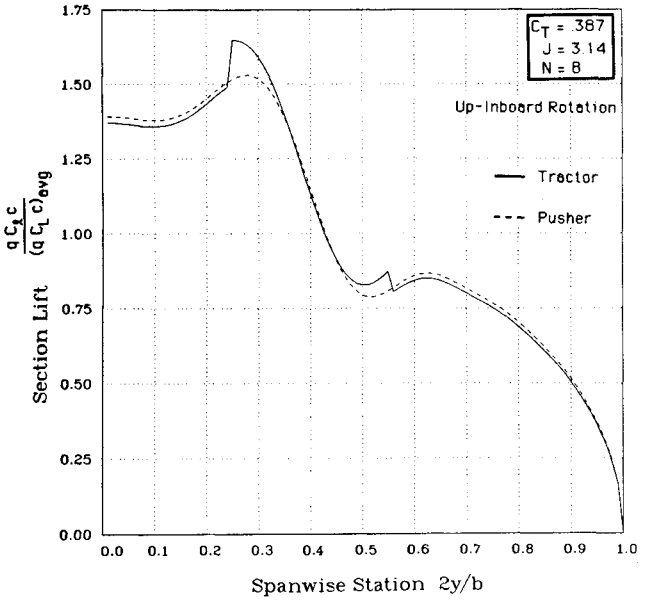

Fig. 4 Optimal wing lift distributions for pusher and tractor installations.

in span loading. Since the slipstream rotation induces changes in the lift distribution in the same sense as required for minimum drag, this design philosophy is certainly superior to one in which the wing is twisted to retain a nearly elliptic distribution and thus achieves no swirl recovery.[2]

However, in general, the lift distribution which minimizes induced drag requires some wing twist. This is especially evident when the propeller is mounted behind the wing. The dashed curve in Fig. 4 shows the lift distribution for minimum drag in this case. As long as the propeller disk cuts the wing wake, it is possible to "preswirl" the flow entering the rotor disk and to recover essentially the same efficiency gain as in the tractor arrangement.

A small difference between these cases is associated with the effect of axial velocities on wing lift. The increased local velocity over the wing reduces the circulation required for a given lift so that the self-induced drag (which depends only on the circulation distribution) is reduced. The axial velocities produce a very small effect on the wing circulation distribution, but tend to increase the section lift in the slipstream and decrease the section lift coefficient based on local dynamic pressure.

Figure 5 compares the optimal distribution of lift for a wing with up-inboard, up-outboard, and counter-rotating propellers. The increase in circulation over areas of the wing affected by slipstream "upwash" are evident.

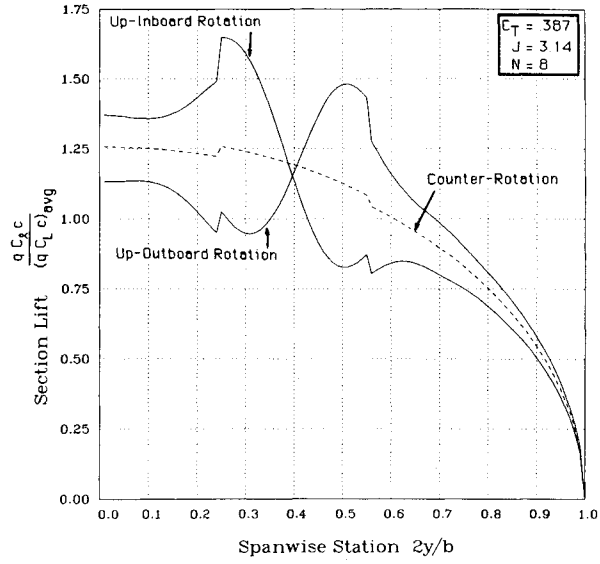

Fig. 5 Optimal wing lift distributions for single- and counter-rotation.

Gains in Propulsive Efficiency

It is apparent from these results that favorable propeller-wing interference resulting in lower induced drag or, equivalently, induced thrust, may be produced by appropriate wing design; but how important is this effect? To what extent can propeller swirl losses be recovered by the wing? Table 1 shows that this inviscid interaction is by no means negligible—most of the swirl loss is recovered by wings with optimal loading. The table shows efficiency losses associated with the propeller and the gains possible from propeller-wing interaction (savings in induced drag are added to the propeller thrust in the computation of effective installed efficiency).

The efficiency losses for a lightly loaded conventional propeller are shown in the first column of Table 1. The effect of finite propeller size (actuator disk theory) is a loss of 2.5% in efficiency; the finite number of blades (4 in this case) brings the loss to 3.2% and the swirl losses bring the total inviscid efficiency loss to 5.6%. In this case, the optimal wing lift distribution provides complete recovery of swirl losses while the effect of increased dynamic pressure increases the efficiency of a tractor arrangement by an additional 0.7%. The net installed (inviscid) efficiency of the tractor arrangement is almost identical to that of the isolated actuator disk.

The efficiency changes associated with a more highly loaded propfan-like arrangement are shown in columns 2, 3, and 4 of the table with up-inboard, up-outboard, and counter-rotating propellers, respectively. The larger swirl loss (7% for these single-rotation designs) is offset by a gain of 5.6% due to interaction of the wing with the up-inboard rotating propeller. The axial velocities in the tractor arrangement provide another small (0.6%) increment.

As expected, the interaction is less favorable for propellers with up-outboard rotation. The reasons for this are apparent from the lift distributions of Fig. 5. In order to take advantage of propeller upwash, the wing circulation must be increased in this region and up-outboard rotation results in a greater departure from an elliptical circulation distribution. A 2.3% efficiency gain due to swirl recovery remins available in this case—less than half of that possible with up-inboard rotation.

Column 4 of the table shows the losses and favorable interaction associated with a counter-rotating system. Similar gains due to axial velocity exist in this case (0.6%), but the opportunity for favorable interaction is, of course, much more limited without slipstream swirl. The net difference in efficiency between single-rotation and counter-rotation systems is thus reduced from 7% for isolated propellers to just over 1% for wing and tractor propeller combinations.

The effect is amplified by increasing wing lift coefficient and reducing aspect ratio. In the above cases an aspect ratio 10 wing at $C_L = 0.5$ has been assumed. If, however, the wing has an aspect ratio of 6 and $C_L = 0.8$, the net installed efficiency of the single-rotation propeller exceeds that of the counter-rotating propeller. In fact, the effective propulsion efficiency is 102%!

This result is contrary to the assertion of Ref. 5 that "The thrust recovery or drag reduction cannot exceed the swirl energy lost in the isolated propfan efficiency." Thrust recovery *may* exceed the swirl loss of an isolated propeller since the wing also exhibits "swirl loss" manifested by the circulation shed in the wake—the optimal solution is one in which a small residual swirl remains in the propeller slipstream, canceling some of the rotational energy in the wing wake. The effectiveness of swirl recovery at more typical cruise conditions is therefore less surprising. (The "perfect" recovery shown in the first column of Table 1 does indeed compensate completely for the swirl loss, but is in no sense "perfect.")

Propeller Location

The propeller's spanwise position plays a small role in wing-propeller interaction, with somewhat greater benefits available as the propeller is moved outboard. These effects are likely overwhelmed by factors such as inertia relief and engine-out performance.

The vertical location of the propeller disk is of greater importance. In addition to reducing the area of the wing affected by the slipstream, the axial inflow velocity is modified when the propeller is located near the wing. However, it is assumed that the propeller axis lies in the plane of the wing for all cases examined here.

The longitudinal position of the propeller has a small effect on net efficiency. Axial induced velocities may reduce wing induced drag slightly, but the major interactions associated with swirl recovery are independent of longitudinal position. The same lift distribution which leads to maximum recovery of swirl losses in the tractor configuration leads to maximum efficiency when the propeller is mounted aft of the wing by "pre-swirling" the flow entering the propeller. The propeller disk must cut through the wake sheet for this interaction to occur.

Discussion

The preceding results, despite obvious limitations associated with the assumptions of ideal fluid flow, have practical implications for the design of wing-propeller systems.

Table 1 Ideal efficiency losses
(Wing $C_L = 0.5$, $y_{prop} = 0.15$, $AR = 10$, $2R/b = 0.15$)

Configuration Rotation	Conventional Up-inboard	Propfan Up-inboard	Propfan Up-outboard	Propfan Counter-rotation
No. of blades	4	8	8	8
Thrust coefficient	0.1	0.387	0.387	0.387
Advance ratio, J	1.57	3.14	3.14	3.14
Actuator disk loss, %	2.5	2.4	2.4	2.4
Tip loss, %	0.7	0.6	0.6	0.6
Swirl loss, %	2.4	6.9	6.9	0
Uninstalled loss, %	5.6	9.9	9.9	3.0
Swirl recovery, %	2.4	5.5	2.3	0
Axial interference, %	0.7	0.6	0.7	0.7
Net installed loss, %	2.5	3.8	6.9	2.3

Propeller Design

The ability of the wing to recover most (if not all) of the swirl losses experienced by the propeller reduces some of the performance advantages of counter-rotating systems. (Cogent arguments are based on mechanical simplicity, structural weight, and viscous or compressibility-related issues.)

The inviscid efficiency of systems with up-inboard rotation exceeds that of propellers with up-outboard rotation; however, even the latter may take advantage of some favorable wing interaction.

The distribution of circulation along the propeller blades is computed here based on the assumption of isolated propeller minimum induced loss. This is not the distribution for maximum isolated efficiency in real, viscous flow, let alone maximum integrated efficiency. The assumption of minimum induced loss propeller design is a reasonable approximation but the optimum propeller will generate greater swirl. One of the more significant effects of propeller geometry on wing-propeller interaction is the propeller diameter, with larger diameter-to-span ratios permitting increased swirl recovery.

Inviscid performance contributes little to the decision between tractor and pusher configurations. Cyclic blade loading in the aft-mounted case and viscous, compressible aspects of propeller slipstream and wing interaction are more critical considerations.

Wing Design

The design of the wing for an efficient integrated propulsion system is affected more by the presence of the propeller than the propeller design is affected by the wing's presence. The wing airfoil shape, twist distribution, and chord must be modified—not to obtain a pressure distribution similar to the clean wing distribution, nor for an efficient power-off span load distribution, but rather to approximate the optimal power-on lift distribution.

The departure of this distribution from the smooth, nearly elliptic, clean wing distribution complicates the wing design, especially at transonic speeds.[2-5] To prevent undesirable viscous or compressibility effects in the region of increased lift coefficients, the section shape must be modified. Reference 3 shows that this may be accomplished by reducing inboard airfoil thickness. However, a reduction of wing thickness has undesirable structural effects, especially near the root. Such structural considerations, together with viscosity-related effects, have led some to consider up-outboard rotation at the expense of much of the swirl recovery.[4] It should be noted, however, that although most studies have been concerned with twist, thickness, and camber modifications, changes in chord distribution have powerful effects on wing performance in this case. Increasing the chord inboard of the nacelle and decreasing it outboard achieves a simultaneous reduction of inboard section C_l and thickness ratio without large structural compromises.

Conclusions

The simplified analysis presented here leads to several fundamental results related to the inviscid interaction of wing-propeller systems:

1) The optimal distribution of wing lift in the presence of a propeller differs significantly from the isolated wing distribution, especially with highly loaded propellers.

2) With this distribution, the wing is capable of restoring much of the loss associated with slipstream swirl. In some cases, all of the loss is recovered, and in certain cases the wing-propeller interaction is such that the efficiency exceeds that of a counter-rotating system.

3) Equal increases in efficiency due to swirl reovery by the wing may be obtained in either tractor or pusher arrangements. In the latter case, the wing "pre-swirls" the flow, leading to an increase in propeller thrust.

References

[1]Glauert, H., "Airplane Propellers," Div. L, *Aerodynamic Theory*, edited by W. F. Durand, Vol. IV, Springer, Berlin, 1935.

[2]Aljabri, A. and Swearengen, J., "Analysis of Mach Number 0.8 Turboprop Slipstream Wing/Nacelle Interactions," NASA CR 166419, Dec. 1982.

[3]Samant, S., Hultman, D., Lines, T., Yu, N., and Rubbert, P., "Analysis and Design of Prop-Fan Nacelle Installations at Transonic Speeds," NASA CR-166376, July 1982.

[4]Vernon, D., Page, G., and Welge, H., "Prop-Fan Experimental Data Analysis," NASA CR 166582, Aug. 1984.

[5]Welge, H., "Prop-Fan Integration at Cruise Speeds," AGARD Paper 6970, May 1981.

[6]Kroo, I., "A General Approach to Multiple Lifting Surface Design and Analysis," AIAA Paper 84-2507, Oct. 1984.

[7]Munk, M., "Minimum Induced Drag of Airfoils," NACA Rept. 121, 1921.

[8]Goldstein, S., "On the Vortex Theory of Screw Propellers," *Proceedings of the Royal Society, London,* Ser. A, Vol. 123, No. 792, April 1929.

[9]Prandtl, L. and Tiejens, O., *Applied Hydro- and Aeromechanics*, Dover, New York, 1934.

[10]Jones, R., "The Spanwise Distribution of Lift for Minimum Induced Drag of Wings Having Given Lift and Root Bending Moment," NASA TN-2249, 1950.